Leaching Model for a Cement Mortar Exposed to Intermittent Wetting and Drying

Andrew C. Garrabrants, Florence Sanchez, and David S. Kosson
Dept. of Civil & Environmental Engineering, Vanderbilt University, Nashville, TN 37235

Numerical simulations of inorganic species release from an intermittently wetted cement material without carbonation effects are presented. The intermittent mass-transport (IMT) model combines previously developed approaches describing constituent diffusion coupled with solid-phase dissolution/precipitation and two-regime drying of a cement matrix stored at constant relative humidity. Model simulations were validated using experimental data showing the effects of intermittent wetting on release of major matrix species (Ca, Na, K, Cl, OH) and pH-dependent trace metals (Cd, Pb). The IMT model successfully describes constituent release flux for intermittent wetting cases with storage in an inert atmosphere (100% N_2) at three levels of relative humidity (23%, 48%, 98% RH). Leachate pH simulation accounted for the release of soluble alkaline salts in conjunction with the dissolution of calcium hydroxide. The release simulations for pH-dependent species were subsequently improved over pH determination based solely on calcium hydroxide dissolution.

Introduction

Over the past thirty years, the role of cementitious materials has expanded from structural building materials (cements and concretes used in the current infrastructure of roads, bridges, and buildings) to include cement-based matrices providing environmental control of hazardous contaminant release. It is now common for potentially hazardous species, including radioactive and chemical wastes, to be immobilized within a cementitious matrix by means of a class of treatment processes known as solidificaton/stabilization (S/S). Typically, the treated materials are disposed in regulated landfills where exposure to the environment can be monitored and controlled (Conner and Hoeffner, 1998). However, a recent shift toward recycling has led to the incorporation of waste and secondary materials into roadbed (Berendsen, 1997; Eighmy et al., 2002) or building materials (Jansegers, 1997; Nishigaki, 2000). The long-term efficacy of the S/S treatment process largely depends on the durability of the treated material in its environmental scenario. Thus, it has become increasingly important to understand and predict the relationship between constituent release and physical durability of the cement matrix. In addition, an understanding of the aging and failure processes that compromise the durability of these materials can be used to improve the performance of future materials.

Long-term durability of cementitious materials is a complex issue that must account for the effect of both internal and external stresses on the cement matrix. Such stresses affect the performance of both structural cements and S/S treated materials in much the same way (Klich et al., 1999). Internal stresses include phenomena originating from within the matrix that affect the long-term morphology of the cement composition. Changes in chemical composition and structure due to internal stresses, for example, migration of metal species from waste aggregates to the cement paste (Klich et al., 1999), usually are material-specific and often are geologically slow (Glasser, 1993). Consequently, the effect of internal stresses is often difficult to study under controlled conditions and typically requires the use of accelerated aging experiments (Eighmy and Chesner, 2001). For many cement or concrete applications, the placement environment may generate external stresses leading to deterioration of the matrix. External stresses may include cycles of freezing and thawing, chemical attack by reactive agents (such as sulfate, chloride, carbonic acid, oxygen), release and depletion of matrix constituents due to leaching, and moisture loss via matrix drying. Deterioration of cementitious materials via external

Correspondence concerning this article should be addressed to D. S. Kosson.

stresses tends to be more dramatic and less kinetically limited than alternation due to internal factors. For example, freeze–thaw cycles have been seen to cause physical damage to monolithic cement matrices by promoting heaving and cracking (Cerný et al., 2001; Eighmy and Chesner, 2001; Klemm and Klemm, 1997). Chloride ingress has been associated with both spalling (Delagrave et al., 1996) and corrosion of reinforcing bars in structural concretes (Dhir et al., 1989; Johannesson, 1999; Kayyali and Qasrawi, 1992). Sulfate attack may lead to expansive cracking and decalcification of cement-based matrices through the production of gypsum and ettringite (Clifton et al., 1995; Klich et al., 1999). Drying of cementitious matrices may cause matrix shrinking (Penev and Kawamura, 1991; Sakata, 1983), increase microcracking (Kjellsen and Jennings, 1996), and facilitate the internal mass transport of reactive gases such as carbon dioxide (Papadakis et al., 1989).

In undersaturated matrices, the reaction of carbon dioxide with components in the pore water leads to conversion of hydroxides to carbonates and overall neutralization of the cement matrix (Lange et al., 1996; Macías et al., 1997; Papadakis et al., 1989, 1991). Carbonation of Portland cement–based wastes also has been associated with increased release of matrix salts (Gervais et al., 2003), increased release of hazardous inorganic constituents such as arsenic (Garrabrants et al., 2003; Sanchez et al., 2001), and decalcification of the matrix (Mollah et al., 1993). Over very long release intervals, decalcification due to leaching of calcium from the matrix has been observed to increase porosity and reduce compressive strength (Carde et al., 1996; Carde and François, 1997a,b; Carde and François, 1999). Matrix alteration resulting from carbonation and constituent release are often-overlooked issues affecting both cement durability and the retention of S/S treatment.

Recent studies indicate that constituent release and carbonation can be enhanced by cycles of intermittent wetting (IW) in which the release from a saturated matrix is interspersed with periods of storage (Garrabrants et al., 2002). During storage intervals, the release process to the surrounding environment is stopped due to the lack of a continuous aqueous-phase external to the matrix. Within the matrix, however, continued mass transport leads to gradient relaxation and redistribution of aqueous species (Sanchez et al., 2003). If the relative humidity of the storage environment is low enough to initiate drying, the redistribution process may be complicated by species precipitation as the relative saturation of the pore structure decreases.

Current models used to assess the release of "constituents of potential concern" (COPCs) from cementitious matrices either assume a continuously saturated matrix (Barna, 1994; Batchelor, 1998; Hinsenveld, 1992; Hinsenveld and Bishop, 1996; Moszkowicz et al., 1994, 1997, 1998; Park and Batchelor, 1999a,b, 2002; Sanchez, 1996; Sanchez et al., 2000) or correct saturated release for intermittent wetting using an empirical correction based on the diffusion theory (Kosson et al., 1996). While, in general, many of these approaches tend to be direct and conservative, the liability associated with infra-structure or waste-treatment failure calls for a more rigorous, predictive modeling approach for intermittently wetted materials. This new modeling approach should be adaptable for a wide range of intermittent wetting scenarios, since material exposure scenarios can vary greatly. The current research presents the formulation and validation of a mathematical model to simulate laboratory release of matrix components and trace metal species from a cementitious material exposed to intermittent wetting and drying. Since this article represents a first attempt to model release under intermittent wetting conditions with drying, alteration of the matrix resulting from chemical reaction with the environment (such as carbonation, sulfate attack, oxidation) is not considered.

Approach

The intermittent mass-transfer (IMT) model was developed from previous models describing (1) constituent mass transport in saturated media (Sanchez, 1996; Sanchez et al., 2003), and (2) moisture/water vapor transport in cementitious materials (Garrabrants and Kosson, 2003). Mass transport under intermittent wetting and drying conditions was simulated as a cyclic pattern of (1) species release from a water-saturated matrix during a leaching period, followed by (2) mass transport within the matrix during a period of storage in an unsaturated environment at constant relative humidity.

The IMT model was used to describe the release of major pore water species (Ca^{2+}, OH^-, Na^+, K^+, Cl^-) and trace metal contaminants (Cd, Pb) from a cement-based waste material for intermittent wetting cases with storage atmospheric relative humidity (RH) at three levels (23%, 48%, 98% RH). In addition to intermittent wetting cases, the release from the matrix during continuous leaching over the same assessment interval was simulated for comparison. In order to match simulations to experimental data from a previous study (Garrabrants et al., 2002), the simulated leaching period was bro-

Table 1. Leaching and Storage Intervals for Intermittent Tank Leaching and Continuous Tank Leaching

Cycle	Continuous Tank Leaching Leaching Intervals (h)	Intermittent Tank Leaching Leaching Intervals (h)	Intermittent Tank Leaching Storage Intervals (h)
1	3 3 6 12 24	3 3 6 12	24
2	6 6 12 24 48	6 6 12 24	48
3	12 12 24 48 96	12 12 24 48	96
4	24 24 48 96 192	24 24 48 96	192
5	48 48 96 192 384	48 48 96 192	384
6	48 48 96 192 384	48 48 96 192	384
	94 days (30 intervals)	47 days (24 intervals)	47 days (6 intervals)
Cumulative time	94 days	94 days	

Table 2. Total Elemental Content of the S/S MeO Matrix

Element		Total Content (mg/kg)	
Aluminum	Al	13,700	±300
Arsenic	As	3,050	±60
Calcium	Ca	217,000	±40,000
Cadmium	Cd	3,100	±100
Chloride	Cl	1,880	±66
Copper	Cu	2,920	±6
Iron	Fe	9,100	±300
Potassium	K	3,400	±100
Sodium	Na	1,610	±25
Lead	Pb	2,700	±7
Sulfur	S	10,700	±110
Zinc	Zn	3,220	±6

ken into discrete intervals for both intermittent wetting and continuous leaching cases as presented in Table 1.

The subject matrix for experimental release data (denoted S/S MeO) was a cement mortar (that is, ordinary Portland cement, sand, and water) containing metal oxide powders (that is, As_2O_5, CdO, CuO, PbO, and ZnO). Total elemental content of the cement matrix as determined by neutron activation analysis and X-ray fluorescence is shown in Table 2. Physical characterization of the cementitous material included bulk porosity (0.13 m^3pore/m^3matrix) and material density (2,200 kg/m^3matrix). A detailed description of the treatment recipe and intermittent wetting experimental conditions is presented elsewhere (Garrabrants et al., 2002). Material-specific data, used to parameterize the model were taken from previous studies and include pore water/material equilibrium information (Garrabrants et al., 2003) and parameters describing moisture transport in the cement matrix (Garrabrants and Kosson, 2003).

Model Formulation

Mass transport within the IMT model was based on the equation of the coupled dissolution–diffusion (CDD) model, developed to describe constituent release from continuously saturated media (Sanchez, 1996). More recently, the CDD model was modified to simulate species release in the case of an intermittently wetted cementitious matrix for which storage occurred without drying or carbonation (Sanchez et al., 2003). In this case, the atmospheric relative humidity during storage intervals was maintained at 100% RH, and storage was characterized as a period of "nonleaching." The intermittent wetting case without drying is a special case because the ambient atmosphere will most likely be less than 100% in many application scenarios; thus, an initially saturated porous matrix will lose moisture to the environment. In order to approximate the changes in matrix saturation as a function of storage environment relative humidity, a moisture-transport model was developed and validated (Garrabrants and Kosson, 2003).

Model assumptions

The current version of the IMT model incorporates the mass-transport phenomena described using the CDD model with the ability to simulate matrix drying during periods of storage. Therefore, many of the assumptions of the CDD model and moisture-transport model are applicable to the IMT approach. In the development of the IMT model, the following principal assumptions are made:

(1) The porous medium of concern is a homogeneous stable skeleton, with solid phases [such as $Ca(OH)_2$, $Pb(OH)_2$] precipitated onto the skeletal surface and a liquid phase initially filling the pore void.

(2) The matrix can be represented by a 1-dimensional (1-D) geometry of thickness $2d$. Thus, there exists an axis of symmetry at $x = d$, where the no-flux boundary condition prevails (Bazant and Najjar, 1971; Sanchez, 1996). At the bulk matrix interfaces, $x = 0$ and $x = 2d$, the material is exposed to environmental conditions.

(3) The matrix is a macroscopically uniform medium at initial conditions. Mass release and dissolution/precipitation phenomena do not significantly alter the porous structure of the matrix (that is, porosity, ϵ, and tortuosity, τ, remain constant) at both the macroscopic and microscopic levels. In addition, the matrix is a fully hydrated, or mature, cement matrix and the loss in moisture content due to continued hydration reactions (self-desiccation) is assumed negligible (Papadakis et al., 1989).

(4) Local equilibrium exists between solid and liquid phases within a differential element. Under this assumption, solid dissolution is considered instantaneous and the equilibrium activity of all pH-dependent species (such as Cd, Pb) can be given by a liquid–solid partitioning curve as a function of solution pH.

(5) Highly soluble species are initially present in the cement matrix as aqueous species only, and no initial solid phase for sodium, potassium, or chloride is considered in this model.

(6) During mass transport, changes in ionic strength and, thus, activity coefficients are assumed negligible over small time intervals and between differential elements.

(7) The system and mass-transport processes are considered isothermal (Šelih et al., 1996) so that the density of the liquid phase (ρ_{liq}) is considered constant and the effect of temperature on the moisture transport is negligible.

(8) Changes in water saturation are considered negligible to the mass-transport process over small time intervals and between differential elements. Thus, for each step in the mass-transport calculation, values of local saturation can be given as a function of drying time using the moisture transport equations.

(9) Within the drying process, local equilibrium exists between liquid and vapor phases within a differential element. During the funicular drying regime, equilibration of capillary pressure is considered instantaneous. In addition, a vapor–liquid desorption isotherm may be used to represent the pore liquid saturation as a function of relative humidity during the isothermal phase of the drying process.

Mass-transport equations

For dissolved species at infinite dilution, it is assumed that ion–ion interactions are negligible and activity may be approximated by the concentration of the species in solution. However, the infinite-dilution assumption is not valid for the high ionic strength solutions ($\sim$2 M) common to the pore

water of cementitious matrices (Batchelor and Wu, 1993). Significant gradients in ionic strength may develop during leaching, either within the matrix during drying or between the bulk matrix and the leachate. In addition, the driving force for mass transport is more closely associated with the gradients in species activity rather than with concentration gradients. Thus, it was important to account for the high ionic strength of the cement matrix by expressing the governing equation of the concentration-based CDD model in terms of species activity.

The governing mass-transport equation in the CDD model is a mass balance relating the rate of accumulation of an aqueous species, k, to the sum of the divergence in the flux in k with respect to spatial coordinate, x, and the generation rate of species k (F_k)

$$\frac{\partial L_k}{\partial t} = D_k^{\text{eff}} \frac{\partial^2 L_k}{\partial x^2} + F_k(L_1, ..., L_N, S_p) \tag{1}$$

The liquid-phase concentration of species k (L_k) in the CDD model is a global variable based on the unit volume of the porous matrix. In order to express Eq. 1 in terms of a pore water, or local, variable such as species activity, the global concentration first is converted to a local concentration in the pore solution (c_k)

$$L_k = c_k \cdot \frac{\epsilon \cdot \theta}{1{,}000} \tag{2}$$

In the preceding equation, the value 1,000 is a lumped unit conversion in terms of mass (10^6 mg/kg) and volume ($m^3_{\text{liquid}}/10^3$ L) assuming unit density of the pore solution. Applying this conversion to Eq. 2 and canceling like terms gives the mass-balance equation in terms of pore solution concentration

$$\frac{\partial c_k}{\partial t} = D_k^{\text{eff}} \frac{\partial^2 c_k}{\partial x^2} + F_k(c_1, ..., c_N, S_p). \tag{3}$$

For species k, a proportion between a mass-based concentration (c_k) and a "mass" activity (a_k) is presented using the activity coefficient (γ_k), which is a function of ionic strength

$$a_k = \gamma_k \cdot c_k \tag{4}$$

By applying the relationship shown in Eq. 4, the mass-balance equation can be expressed as a function of species activity

$$\frac{\partial a_k}{\partial t} = D_k^{\text{eff}} \frac{\partial^2 a_k}{\partial x^2} + F_k(a_1, ..., a_N, S_p). \tag{5}$$

In a similar manner, the first-order expression for the generation rate of species k due to dissolution/precipitation reactions can be converted from a global variable in terms of L_k to an activity expression in terms of a_k, where

$$F_k = \beta_k(a_k - a_k^{\text{eq}}) \qquad \text{if } S_p > 0 \tag{6a}$$

and

$$F_k = 0 \qquad \text{if } S_p = 0 \tag{6b}$$

or the species k is not provided by the dissolution of S_p. For pH-dependent species (Cd, Pb), the equilibrium activity, a_k^{eq}, is expressed as a function of local pore water pH using a regressed relationship of experimental equilibrium data (Garrabrants et al., 2003). This experimental solubility approach is similar to that of Kim and Batchelor (2001) and an alternative approach to that of other models employing coupling transport simulations with geochemical speciation modeling. In the IMT model, the equilibrium activity of highly soluble species (Na^+, K^+, Cl^-) is set to a constant, minimal value, ensuring that the initial total species concentration is solubilized. The use of a minimal equilibrium activity allows for potential precipitation during periods of drying.

Generation of species k in the liquid phase is provided by the dissolution of one or several solid-phase components (S_p) containing species k. The continuity equation for the global concentration of these solid phases is expressed in terms of a change in activity of species k in the pore solution

$$\frac{\partial S_p}{\partial t} = \frac{M_p}{M_k} \cdot \frac{\epsilon \cdot \theta}{\gamma_k \cdot 1{,}000} \cdot \beta_k(a_k - a_k^{\text{eq}}) \tag{7}$$

Throughout the model simulation, Eqs. 5 through 7 are solved simultaneously in order to describe constituent transport through the liquid phase.

Initial Condition. The composition of the pore solution is initially in local equilibrium with the solid phase. According to the CDD theory, initial pore water pH is provided by the dissolution constant of calcium hydroxide. Thus, the initial activity of sparingly soluble species is given by the equilibrium activity value at the inital pore water pH of the matrix

$$a_k|_x = a_k^{\text{eq}} \qquad \text{for all } x,\ t = 0 \tag{8a}$$

$$S_p|_x = S_p^o \qquad \text{for all } x,\ t = 0 \tag{8b}$$

Boundary Conditions. At the bulk solid interface with the leaching solution, a material balance within the leaching solution provides the boundary condition for species release

$$V_l \frac{\partial a_{k,l}}{\partial t} = \sigma \cdot \epsilon \cdot D_k^{\text{eff}} \left.\frac{\partial a_k}{\partial x}\right|_{x=0} \tag{9}$$

When the intermittent wetting cycle switches from leaching to storage, the boundary conditions of the model are changed to account for periods of nonleaching. Since there is no continuous leaching phase external to the matrix during storage, the release boundary conditions are represented by a zero flux of species activity

$$\left.\frac{\partial a_k}{\partial x}\right|_{x=0} = 0 \tag{10}$$

At the axis of symmetry ($x = d$), "no flux" conditions hold

throughout the mass-transport process

$$\left.\frac{\partial a_k}{\partial x}\right|_{x=d} = 0 \tag{11}$$

pH Determination. A key assumption of the CDD modeling approach is that pore water pH is controlled by the dissolution of portlandite, $Ca(OH)_2$, coupled with the mass transport of hydroxide ions. At any local point in the matrix, the pore solution is determined by solving a charge-balance equation between the activity of major cations (Ca^{2+}, H^+) and anions (OH^-)

$$0 = 2\cdot\{Ca^{2+}\} + \{H^+\} - \{OH^-\} \tag{12a}$$

In the electroneutrality equation (Eq. 12a), the activity of H^+ can be expressed in terms of hydroxide ion using the dissociation constant of water ($K_a^{H_2O}$)

$$0 = 2\cdot\{Ca^{2+}\}\{OH^-\} + K_a^{H_2O} - \{OH^-\}^2 \tag{12b}$$

The local pH value is determined by solving the second-order equation in terms of $\{OH^-\}$ (Eq. 12b) using the quadratic formula.

An alternate approach for determining pore water pH is made by correcting the CDD determination for the presence of soluble alkaline salts. Since the solubility and transport properties of sodium and potassium are similar, the activity of sodium- and potassium-based alkaline salts can be lumped together and represented as a bulk species activity $\{X\}$. The transport of the bulk alkaline salt species is approximated using the diffusivity and molar mass of potassium. The electroneutrality equation was revised to include the alkaline salt term

$$0 = 2\cdot\{Ca^{2+}\} + \{H^+\} + \{X\} - \{OH^-\} \tag{13a}$$

In the electroneutrality equation, the dissolution of calcium hydroxide can be represented by the kinetic solubility constant for portlandite ($K_{sp}^{Ca(OH)_2}$) and the activity of $\{OH^-\}$ ions

$$0 = 2\cdot K_{sp}^{Ca(OH)_2} + K_a^{H_2O}\{OH^-\} + \{X\}\{OH^-\}^2 - \{OH^-\}^3 \tag{13b}$$

Equation 13b is solved in the model code using the Newton–Raphson method (Carnahan et al., 1969; Constantinides, 1987) for a third-order polynomial in terms of $\{OH^-\}$. Where the local solid calcium phase is depleted, the calcium hydroxide dissolution term reverts to the activity of calcium ion in the pore solution $\{Ca^{2+}\}$, and the expression (Eq. 13a) is solved using the quadratic formula.

Moisture transport (drying) in cement matrices

The drying model for porous media allows for a two-regime drying mechanism dominated by mass transfer of water vapor under (1) external control (funicular drying regime), and (2) internal control (isothermal drying regime). Development and validation of the drying model are presented elsewhere (Garrabrants and Kosson, 2003).

Funicular Drying Regime. For an initially saturated matrix stored in an unsaturated environment at relative humidity less than 100%, the drying process is initially controlled by the flux of water vapor away from the surface

$$J|_{x=0} = \eta(H_{surf} - H_{amb}) \tag{14}$$

The evaporation of liquid water at the surface creates a gradient in capillary pressure that is equilibrated by bulk motion of liquid water. This moisture transfer phase, called the funicular drying phase (Rogers and Kaviany, 1992), is characterized by a flat profile of relative saturation across the matrix due to the rapid equilibration of internal capillary pressure. Uniform drying in cementitious materials has been observed by several researchers (Bentz and Hansen, 2000; Šelih et al., 1996). The change in relative saturation (θ) of the matrix is determined by the flux of water vapor away from the bulk solid surface

$$\frac{\partial\theta}{\partial t} = \frac{\eta(H_{surf} - H_{amb})\cdot\sigma}{\rho_{liq}\cdot\epsilon\cdot\theta^0\cdot V} \tag{15}$$

During this funicular phase, the local value of relative humidity within the matrix remains unity between the bulk solid interface at $x = 0$ and the axis of symmetry at $x = d$

$$H_i = 1 \qquad 0 \le x \le d \qquad \bar{\theta} > \theta_{cap} \tag{16}$$

Isothermal Drying Regime. During the isothermal drying regime, the primary resistance to moisture transfer is internal to the matrix, the mechanism for moisture transport is the diffusion of water vapor, and the liquid saturation is assumed in equilibrium with the vapor phase. Thus, the local value of saturation (θ_i) is given as a function of the local humidity in the pore vapor (H_i) using a liquid–vapor isotherm. For the S/S MeO matrix, the equation for the liquid–vapor isotherm was experimentally determined to be a polynomial in terms of relative humidity (Garrabrants and Kosson, 2003)

$$\theta_i = -0.239 + 2.67\cdot H_i - 1.98\cdot H_i^2 + 0.472\cdot H_i^3 \tag{17}$$

Moisture transport during the transitional period and internal control phase can be well described as the diffusion of water vapor using the parameter for relative humidity in the pore vapor

$$\frac{\partial H}{\partial t} = D_H^{obs}\frac{\partial^2 H}{\partial x^2} \tag{18}$$

The observed diffusivity of water vapor (D_H^{obs}) is empirically expressed as a function of the local relative humidity in the form of an S-shaped curve (Bazant and Najjar, 1971, 1972)

$$D_H^{obs} = D_{100\%}^{obs}\left[\alpha_o + \frac{1-\alpha_o}{1+\left(\frac{1-H}{1-h_c}\right)^n}\right] \tag{19}$$

The function shown in Eq. 18 allows for calculation of effective diffusivity throughout the transition period between funicular and isothermal drying, asymptotically approaching a constant value when the relative humidity approaches that in equilibrium with insular saturation (θ_{ins}). At insular saturation, the liquid phase becomes discontinuous and moisture transport occurs only through the vapor phase.

Initial Condition. The initial moisture conditions for the developed moisture model are that of a fully saturated matrix. Hence, the pore vapor relative humidity is not defined, since a vapor space cannot exist in liquid-filled pores

$$\theta|_x = 1 \qquad \text{for all} \quad x,\ t = 0 \tag{20a}$$

$$H|_x \text{ is not defined} \qquad \text{for all} \quad x,\ t = 0 \tag{20b}$$

Boundary Conditions. In the funicular drying regime, the flux of water vapor away from the matrix surface is related to a uniform decline in mean matrix saturation and a constant relative humidity within the matrix. Thus, the boundary conditions reflect an unsaturated environment and a constant relative humidity

$$\theta|_{x=0} = 0 \tag{21a}$$

$$H|_{x=0} = H_{surf} \tag{21b}$$

When the mean saturation of the matrix reaches the capillary saturation (θ_{cap}), moisture transport away from the interface becomes the boundary condition for the diffusion of water vapor

$$D_H^{obs} \left.\frac{\partial H}{\partial x}\right|_{x=0} = \eta(H_{surf} - H_{amb}) \tag{22}$$

At the axis of symmetry ($x = d$), no-flux conditions hold throughout the isothermal drying process

$$\left.\frac{\partial H}{\partial x}\right|_{x=d} = 0 \tag{23}$$

Numerical method

The equivalent length (d) of the 1-D matrix was descritized into m slices. The partial differential governing equations for activity transport (Eqs. 5 and 7) and moisture transport (Eqs. 15 and 18) were converted to arithmetic equations using a fully implicit central difference scheme in space and Euler's time marching method (Carnahan et al., 1969; Constantinides, 1987; Patankar, 1980). Central difference equations for each local point, i, from the surface of the matrix at $x = 0$ to the axis of symmetry at $x = d$ yielded an overall system of m equations

$$\{A\}[x] = [b] \tag{24}$$

Equation 24 is solved using the method of Thomas (Patankar, 1980) for the unknown vector of values at the next time step, $t = t + dt$.

Model variables and fitting criterion

The majority of the model parameters were set from the experimental results of a previous study, including (1) total or available content of each species (Garrabrants et al., 2002), (2) species equilibrium activity as a function of pH (Garrabrants et al., 2003), and (3) material-specific parameters for the observed diffusivity of water vapor (Garrabrants and Kosson, 2003). The only fitting parameter used to correlate simulations to the experimental leaching data was the effective diffusivity for each species (D_k^{eff}). In general, the effective diffusivity was regressed for a single release case (intermittent wetting interspersed with drying at 23% RH) and then applied to simulate release for all other cases. Thus, independent data sets were used for model calibration and verification.

The selection of a "good fit" was determined by minimizing the result of a characteristic fitting function based on the sum of the residual square errors (Johnson and Bhattacharyya, 1992). First, the sum of the residual square errors for each intermittent wetting cycle j ($SRSE_j$) was calculated using the log transform of the flux data at each matrix location i

$$SRSE_j = \sum_{i=1}^{n} \left\{ \frac{\left[\log(y_{i,exp}) - \log(y_{i,sim})\right]^2}{\left[\log(y_{i,exp})\right]^2} \right\} \tag{25}$$

Next, an overall fit statistic ($SRSE_{sim}$) was formed using a weighted sum of the $SRSE_j$ values from all intermittent wetting cycles and a cycle weighing function (w_j) expressed as the ratio of intermittent wetting (IW) cycle time to the total simulation time

$$SRSE_{sim} = \sum_{j=1}^{6} \{w_j \cdot SRSE_j\} = \sum_{j=1}^{6} \left\{ \left(\frac{t_j}{t_{sim}} \right) \cdot SRSE_j \right\} \tag{26}$$

Experimental Data Preparation

Experimental release information used to parameterize and verify the IMT model included: (1) the tank-leaching data under intermittent wetting conditions (Garrabrants et al., 2002) used to validate the model output, and (2) the equilibrium leachate data (Garrabrants et al., 2003) used in the IMT model to represent the solid–liquid equilibrium. Measured experimental data were expressed in terms of species mass activity in the leachate ($a_{k,l}$) for either comparison with IMT model output or use within the IMT mass transport model. The activity of species k in the leachate ($a_{k,l}$) was calculated using the activity coefficient (γ_k) as a function of ionic strength (I) and the measured leachate concentration ($c_{k,l}$)

$$a_{k,l} = \gamma_k \cdot c_{k,l} \tag{27}$$

Adjustment of experimental data to species activity allowed for a simplification of the mass-transport simulation, so that the number of simultaneously solved liquid-phase species in the IMT model was minimized.

The ionic strength of each leachate was determined by summing up the charge contributions of the major pore species k (that is, Ca^{2+}, Na^+, K^+, Cl^-, OH^-) present in

solution

$$I = \frac{1}{2} \sum_k c_{k,l} \cdot z_k^2 \tag{28}$$

In this analysis, the contributions of trace species (such as Pb, Cd) to the ionic strength are assumed insignificant and could be neglected.

A relationship between ionic strength and activity coefficient was required in order to correct measured concentrations to activity values. Theoretically, an ion-interaction model would be the most robust approach for calculating an accurate mean activity coefficient for the high ionic strength solution of the cement material. For example, the Pitzer ion-interaction approach (Pitzer, 1979) has been applied to calculate mean activity coefficients in cement pore water for diffusion-based release models (Batchelor and Wu, 1993). However, this approach often requires assumptions on the formation of specific mineral species in equilibrium with the pore water. While some simplifying assumptions can be made, the speciation of several cementitious mineral phases is not clearly defined due to the complex chemistry of S/S systems (Batchelor and Wu, 1993; Cocke, 1993; Conner, 1990; Mollah et al., 1995). Therefore, single-ion activity coefficients were calculated by extending the Davies equation for higher ionic strength solutions using activity coefficient as a function of ionic strength data found in the literature (Morel and Hering, 1993).

The Davies equation (Eq. 29) relates single-ion activity coefficients to the ionic strength of electrolyte solutions using the following expression

$$\ln \gamma_k = -A \cdot z_k^2 \left(\frac{\sqrt{I}}{1+\sqrt{I}} \right) - B \cdot I \tag{29}$$

Although it is noted that the Davies equation is typically considered accurate only for weak electrolyte solutions ($I < 0.5$ mol/L), Morel and Hering (1993) have reported data for the Davies equation up to an ionic strength of 4 M. Thus, an extended fit of the Davies equation for higher ionic strength solutions was used within the IMT model. In the case of dilute solutions or natural waters, the parameters A and B have been reported to be 0.5 and 0.2, respectively (Stumm and Morgan, 1996); however, when the Davies equation was fitted to the tabulated data of Morel and Hering (1993), the regressed values were found to be $A = 1.0$ and $B = 0.16$.

Results and Discussion

Leachate pH simulation

A comparison of leachate pH data from the experimental tank-leaching test and simulated leachate pH from the IMT model is presented in Figure 1. The comparison is shown on a logarithmic time scale in order to expand short-term values. Under the assumption that only calcium hydroxide dissolution controls solution pH, the IMT model predicts lower leachate pH values than measured in the experimental leachates, as shown by the broken or dashed lines in Figure 1. Underestimation of the pH is especially evident at the beginning of the experimental data, and corresponds to an er-

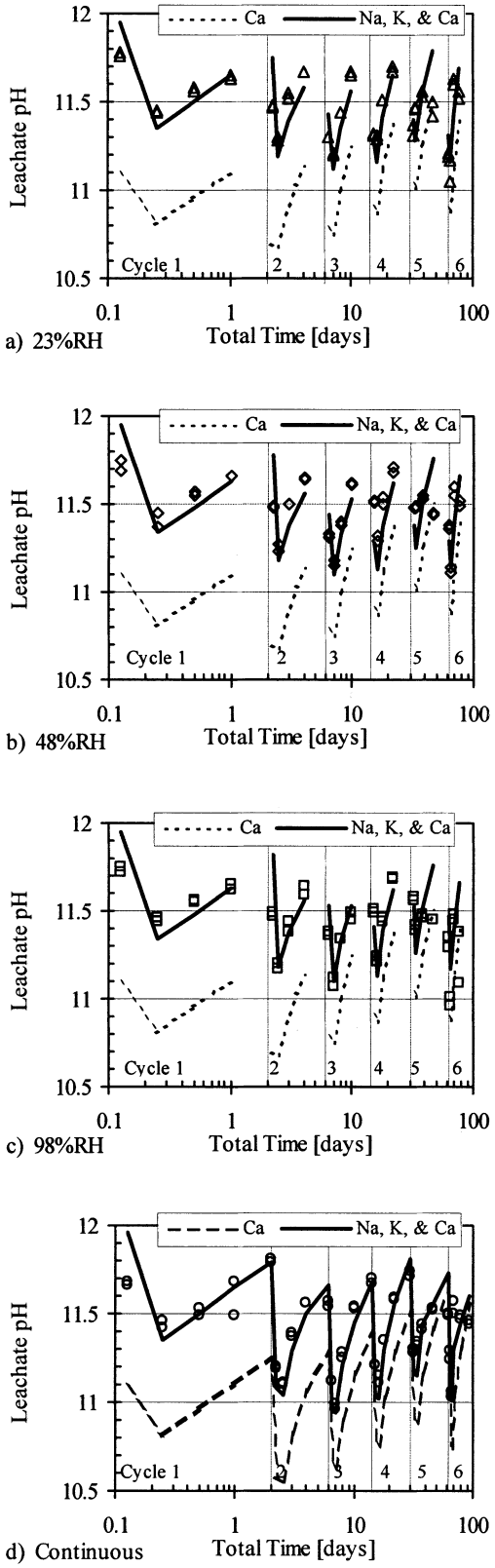

Figure 1. Comparison of leachate pH for experimental data, IMT simulation given by calcium (dashed line), and IMT simulation (solid line) based on alkaline salts and calcium.

(a) 23% RH, (b) 48% RH, (c) 98% RH, (d) continuous leaching.

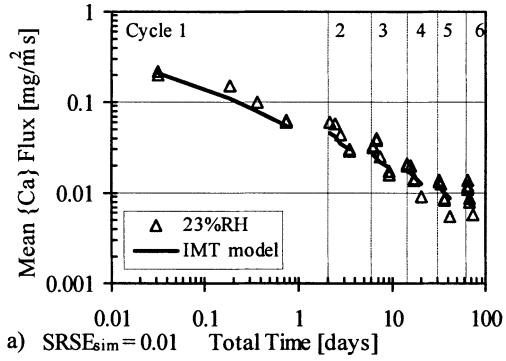

a) $SRSE_{sim} = 0.01$

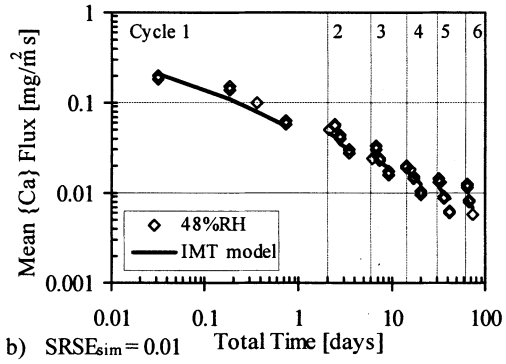

b) $SRSE_{sim} = 0.01$

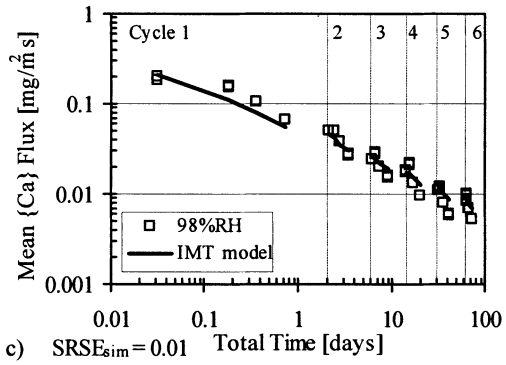

c) $SRSE_{sim} = 0.01$

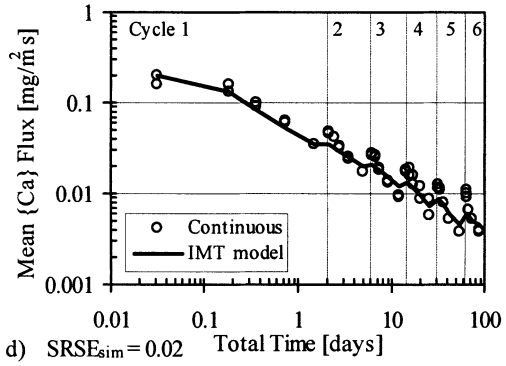

d) $SRSE_{sim} = 0.02$

Figure 2. Comparison of calcium flux ($mg/m^2 \cdot s$) for experimental data and IMT simulation when calcium solubility is a function of solution pH.

(a) 23% RH, (b) 48% RH, (c) 98% RH, (d) continuous leaching.

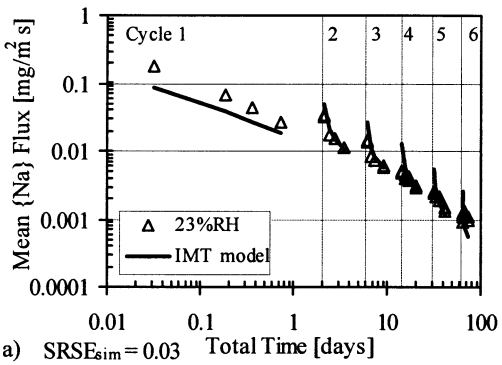

a) $SRSE_{sim} = 0.03$

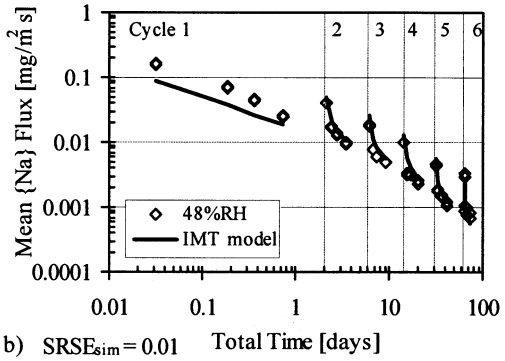

b) $SRSE_{sim} = 0.01$

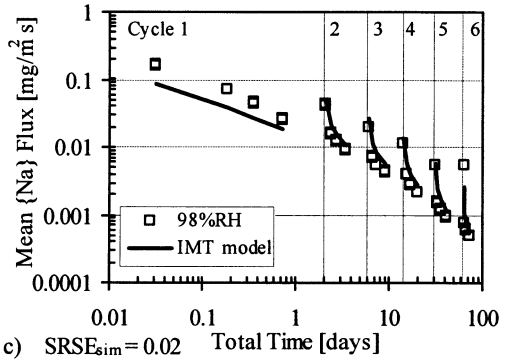

c) $SRSE_{sim} = 0.02$

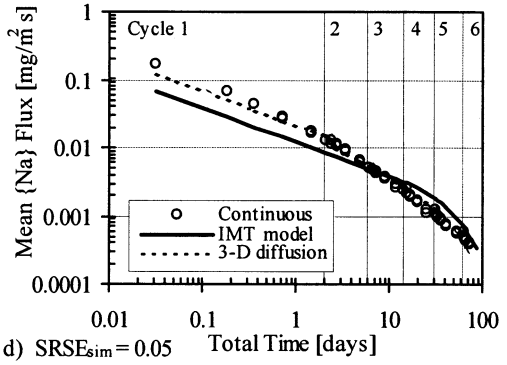

d) $SRSE_{sim} = 0.05$

Figure 3. Comparison of sodium flux ($mg/m^2 \cdot s$) for experimental data and IMT simulation.

(a) 23% RH, (b) 48% RH, (c) 98% RH, (d) continuous leaching.

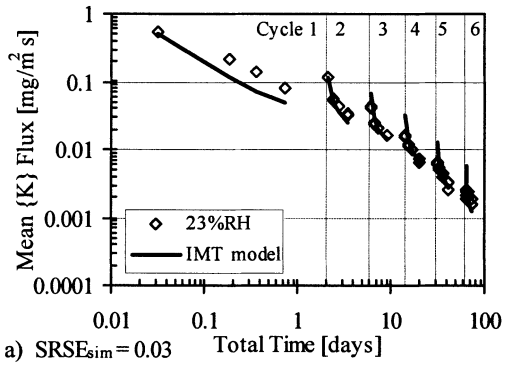

a) $SRSE_{sim} = 0.03$

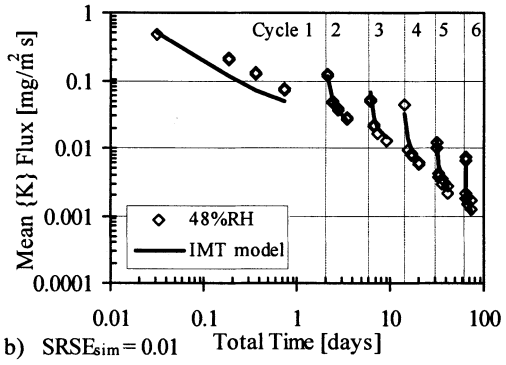

b) $SRSE_{sim} = 0.01$

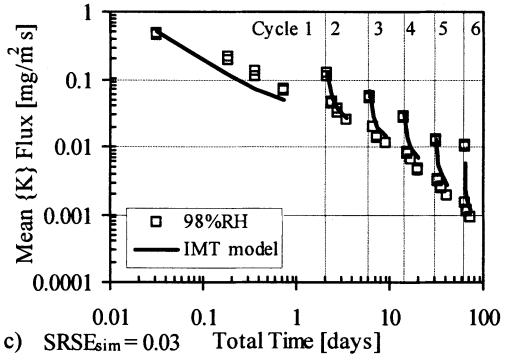

c) $SRSE_{sim} = 0.03$

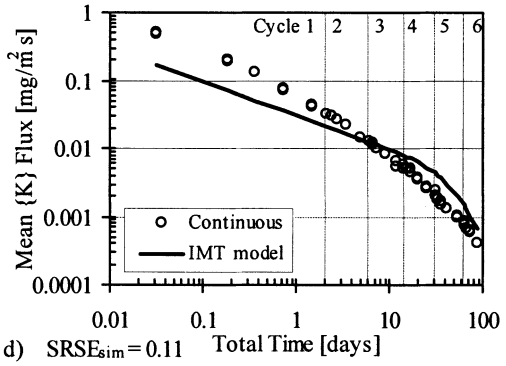

d) $SRSE_{sim} = 0.11$

Figure 4. Comparison of potassium flux (mg/m²·s) for experimental data and IMT simulation.

(a) 23% RH, (b) 48% RH, (c) 98% RH, (d) continuous leaching.

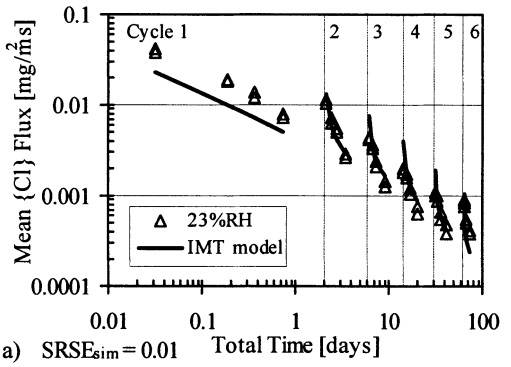

a) $SRSE_{sim} = 0.01$

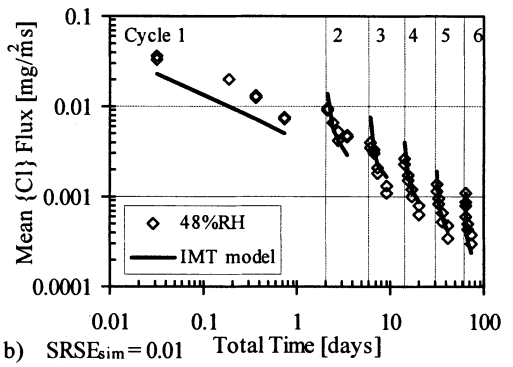

b) $SRSE_{sim} = 0.01$

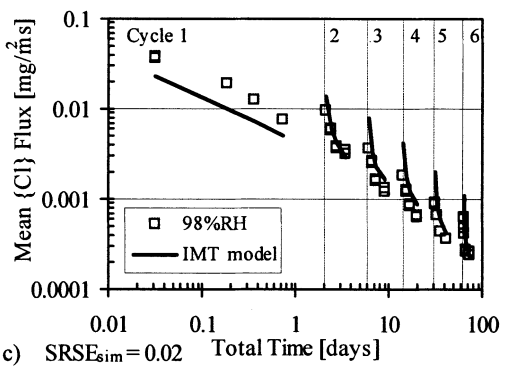

c) $SRSE_{sim} = 0.02$

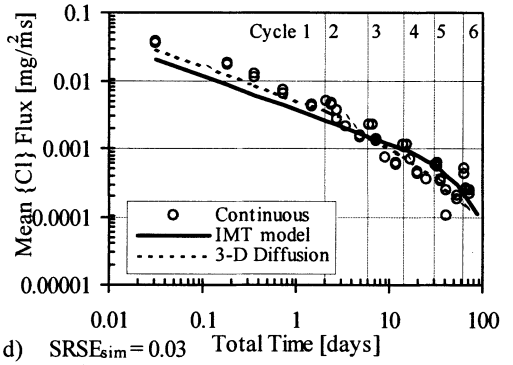

d) $SRSE_{sim} = 0.03$

Figure 5. Comparison of chloride flux (mg/m²·s) for experimental data and IMT simulation.

(a) 23% RH, (b) 48% RH, (c) 98% RH, (d) continuous leaching.

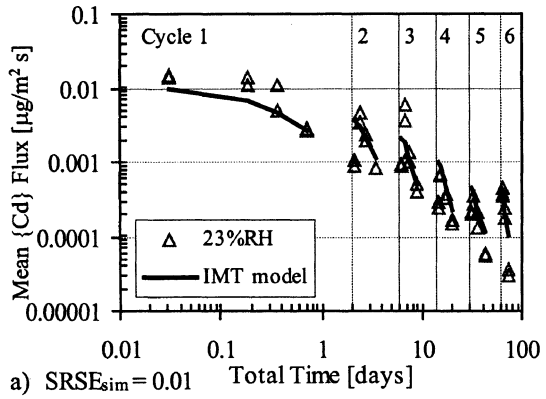

a) $SRSE_{sim} = 0.01$

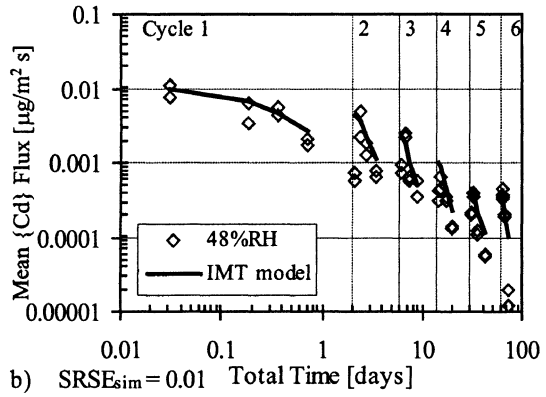

b) $SRSE_{sim} = 0.01$

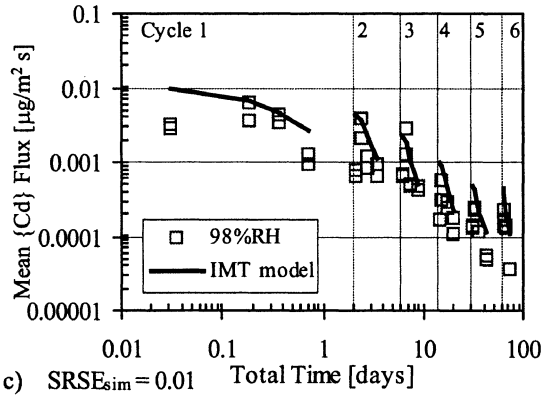

c) $SRSE_{sim} = 0.01$

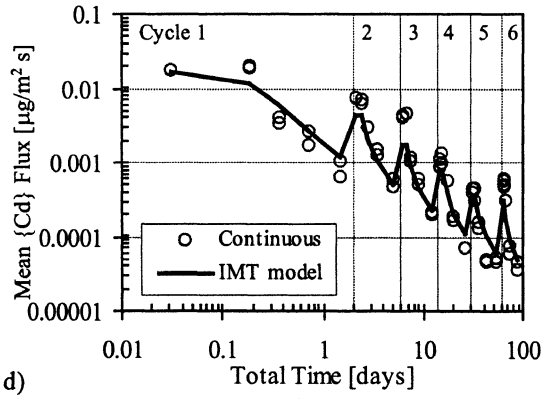

d)

Figure 6. Comparison of cadmium flux ($\mu g/m^2 \cdot s$) for experimental data and IMT simulation.

(a) 23% RH, (b) 48% RH, (c) 98% RH, (d) continuous leaching.

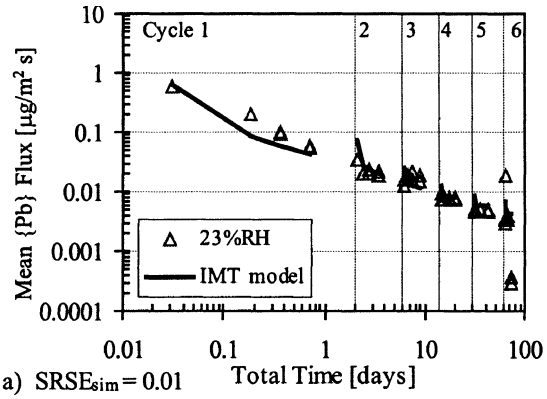

a) $SRSE_{sim} = 0.01$

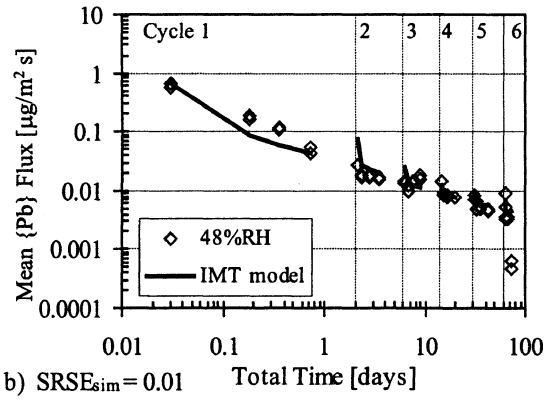

b) $SRSE_{sim} = 0.01$

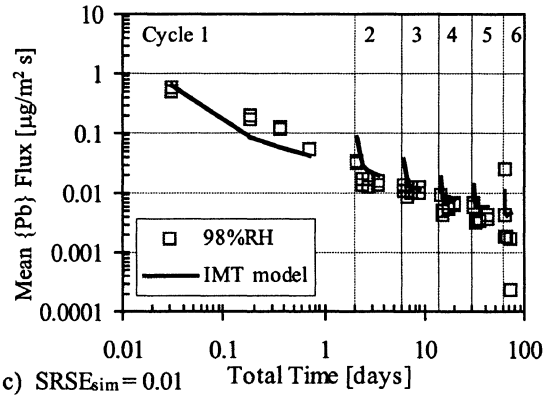

c) $SRSE_{sim} = 0.01$

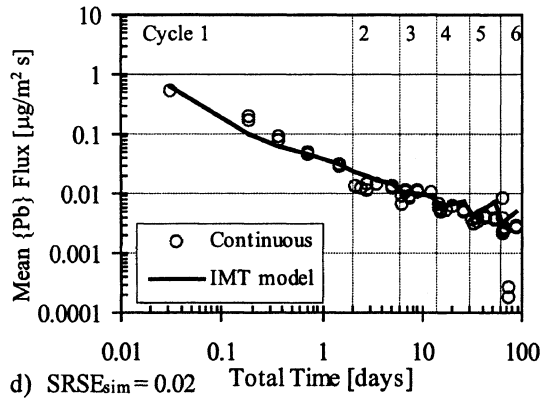

d) $SRSE_{sim} = 0.02$

Figure 7. Comparison of lead flux ($\mu g/m^2 \cdot s$) for experimental data and IMT simulation.

(a) 23% RH, (b) 48% RH, (c) 98% RH, (d) continuous leaching.

ror in predicting hydroxide ion activity in the first leaching cycle of approximately half an order of magnitude. This pH discrepancy would not affect the mass transport of the highly soluble species, since solubility was not considered a function of solution pH. However, many inorganic hazardous waste constituents (such as heavy metals) exhibit solubility behavior that is strongly dependent on solution pH. The error in pH simulation when applied to cementitious materials containing pH-dependent COPCs could lead to significant errors in predicting species release.

Additional sources of hydroxide that could be present in the cementitious pore water include alkaline salts (such as NaOH, KOH). These minerals normally are not considered as significant components of cement clinkers as far as predictions of pore water pH are concerned. For the S/S MeO material, the total potassium content and the fraction of the total sodium content not added to the treatment recipe as NaCl was assumed speciated in the matrix as soluble hydroxides. These species then would contribute to pore water alkalinity in the initial equilibrium and until these hydroxide species were depleted. Also shown in Figure 1 is the simulation for leachate pH from the IMT model after adjusting the mechanism of pH calculation to include alkaline salts (solid line). In general, a much better fit of the pH data is evident for all cases. Under the assumption that alkaline salts control the solution pH within the cementitious matrix at the beginning of leaching, the simulated leachate pH values were within 0.2 pH units of the experimental data. During the later IW cycles, when the alkaline salts began to deplete, the leachate pH coincided with the values given by the dissolution of $Ca(OH)_2$ alone.

Ionic strength

The initial ionic strength in the pore solution was approximately 2 M and was dominated by the presence of highly soluble species, especially sodium and potassium. As these species were released from the matrix, the contribution of pore water pH to the ionic strength becomes more important. Also, during the leaching phase of an intermittent wetting cycle, the pore ionic strength near the surface approached that of the surrounding aqueous phase ($\sim$0.2 M), which was 1/10 that of the bulk matrix ionic strength. Continued mass transport during periods of storage resulted in the relaxation of ionic-strength gradients, observed as an increase in the local ionic strength of the pore solution near the surface of the matrix and a decrease in ionic strength of the pore solution at the matrix core.

The overall effect of gradient relaxation was a progressive decrease in the mean ionic strength of the pore solution with each successive intermittent wetting cycle. The mean ionic strength dropped by a factor of 2 from the initial value after the third storage interval, and by a factor of 10 after the sixth storage interval. These observations give some indication of the dynamic nature of pore-solution ionic strength during mass transport in porous materials with initially high ionic strength. In addition, these observations provide validation to the use of activity rather than mass concentration in the IMT model.

Simulated species release and gradient relaxation

Simulations of constituent release are presented as the mean flux of mass activity (a_k) over the leaching interval as a function of time (shown in Figure 2 through Figure 7). Each of these figures has four panels of output data: the first three panels, (a)–(c), showing a simulated flux for each of the three intermittent wetting cases with storage at 23%, 48%, and 98% RH, respectively, and the last panel, (d), showing the same for the case of continuous leaching. The $SRSE_{\text{sim}}$ for each simulation is indicated in each figure, and the model parameters (such as available content, effective diffusivity) for each species are presented in Table 3.

Gradient relaxation over the duration of the intermittent wetting storage interval was simulated using the IMT model for major pore water and trace metal species. Figure 8 shows liquid-phase profiles of the mass activity (mg/L) of calcium, sodium, potassium, and chloride as a function of dimensionless depth into the 1-D matrix. Figure 9 shows both liquid-phase mass activity (mg/L) and solid-phase concentration (g/m^3_{matrix}) profiles for cadmium and lead as a function of dimensionless matrix depth. Data labels in these figures denote profiles plotted at the end of leaching periods (L#) or storage periods (S#), with numbers indicating the IW cycle number (Table 1) corresponding to each profile. The initial liquid activity level is shown for comparison. All profiles are shown for the case of intermittent wetting with storage at 23% RH.

Calcium. Calcium was considered the primary solid-phase component due to the abundance of calcium hydroxide solid

Table 3. COPC Parameters Used in Simulating Release from the S/S MeO Matrix

COPC	Total Content* (kg/m^3)	Available Content (kg/m^3)	Pore Water Solubility (mg/L)	Effective Diffus. ($D_{\text{eff}} \times 10^{10}$) ($m^2/s$)	Molec. Diffus. ($D_m \times 10^{10}$) (m^2/s)**
Calcium	476	159	Func. of pH†	0.36	7.92
Sodium	3.54	3.54	1.45††	0.058	13.3
Potassium	8.60	8.6	1.9††	0.11	19.6
Chloride	4.14	0.8	0.68††	0.057	20.3
Lead	6.7	6.7	Func. of pH†	0.0078	9.45
Cadmium	6.7	6.7	Func. of pH†	6.30	7.19

*Determined by neutron activation analysis (Landsberger, 1993).
**Tabulated (Lide, 1996).
†Liquid–solid partitioning equation (Garrabrants et al., 2003).
††Set to minimum for total available content dissolution at initial conditions.

(that is 159 kg/m^3_{matrix}), as shown in Table 2. Based on total content as measured by neutron activation analysis, the matrix consists of 21 wt % calcium (Garrabrants et al., 2002).

The comparison of experimental data and IMT simulations for calcium is presented in Figure 2. A single effective diffusivity value could be used to model the flux of mass activity from the S/S MeO matrix for the three intermittent wetting cases and the continuous leaching case. The experimental data exhibits a "cycling" pattern of flux that has been associated with relaxation of the species activity gradient for pH-dependent species during storage intervals (Garrabrants et al., 2002). This pattern is evident within each intermittent wetting cycle shown in Figure 2 by the flux progressing from considerably higher values at the beginning of leaching to lower values at the end of leaching. Prior to the pH correction for the presence of alkaline salts, the IMT model tended to smooth out, or average, the fluctuations in the calcium flux graph rather than simulate them. When alkaline salts control solution pH and suppress calcium solubility, the IMT simulation, $SRSE_{sim}$, values indicate a good and consistent fit of the experimental calcium release data for all cases. Thus, the flux of calcium as shown in Figure 2 indicates that local calcium activity is a function of local pH gradients and follows the solubility behavior shown in the pore-solution equilibrium study (Garrabrants et al., 2003).

The simulated activity profile for calcium, shown in Figure 8a, indicates that the activity is linear in the region where the solid calcium has been depleted and consistent with pore water pH when solid calcium exists. This behavior was expected, since calcium release is strongly influenced by local dissolution and depletion of the solid phase. Relaxation of calcium gradients was nearly immediate, as shown by constant and repetitive storage pofiles for each leaching cycle. The relaxed profiles tend to overlap due to the abundance of solid-phase calcium in the matrix and the model assumption that calcium equilibrium is controlled by the dissolution of $Ca(OH)_2$.

Sodium. In the case of the sodium release, the IMT model was able to simulate the cycling effect shown by the mean flux of sodium activity (Figure 3). Again, a single regression parameter for the effective diffusivity was able to simulate the release of sodium for all three intermittent wetting cases with good agreement. This is especially significant because of the dynamic nature of the cycle fluctuation in comparison to calcium. However, when the IMT model was used to simulate the release of sodium under the conditions of continuous leaching, the model fit was not visually good, despite the reasonable $SRSE_{sim}$ statistic.

Figure 3d shows a comparison between (1) experimental sodium flux data, (2) the IMT model fit, and (3) the sodium flux output of a 3-dimensional (3-D) diffusion model (Barna, 1994). Simulation of experimental data using the 3-D diffusion model was presented in a previous study (Sanchez et al., 2003). The 3-D diffusion model provides a better representation of the experimental flux data, because it better simulates the depletion of species from the matrix. During the continuous leaching experiment, more than 70% of the total content of sodium was released over the duration of the leaching experiment (Garrabrants et al., 2002). The comparison of sodium flux simulations between 1-D and 3-D models indicates that geometry effects (such as edge depletion) are most likely significant when describing the release of highly soluble species from small experimental samples of the S/S MeO matrix.

Since sodium was considered a highly soluble species, it was totally dissolved at the initial conditions and no solid-phase sodium was presented to influence mass transport. Thus, Figure 8b shows that the leaching profiles are not linear like those of calcium, but curve as the sodium profile nears the surface. The sodium profile approaches the initial condition of the start of the leaching period at the center of the matrix. Note the change in scale of the profile from the calcium graph due to the relatively deep penetration of the mass-transfer profile for sodium. During storage, relaxation of the activity gradient for sodium is nearly completed after the shortest experimental storage duration of 24 h (S1). Figure 8b shows that the pore water concentration decreases with subsequent leaching. For example, sodium mass release and relaxation during IW Cycle 1 resulted in a decrease in the liquid activity profile from the inital condition of 27,000 mg/L to an equilibrated profile of 23,300 mg/L (S1). The relaxed sodium profile continued to decrease with each subsequent IW cycle until a uniform concentration of 1,550 mg/L (S6) was established at the end of IW Cycle 6.

The sodium gradient relaxation shown in Figure 8b indicates that after a relatively short storage interval, the pore water activity profile of sodium essentially becomes flat for each leaching cycle at a level that is directly related to the mass released in previous leaching periods. The initial conditions for mass transport at the beginning of the leaching phase of the intermittent wetting cycle is that of a uniform species. The gradient relaxation pattern explains why the 1-D IMT model was able to simulate release from the intermittent cases, where depletion effectively did not occur, but was inadequate for describing release for continuous leaching, where depletion occurred. In this context, a simplified description of the release of highly soluble species from intermittently wetted cement matrices potentially may be made using a series of analytical semi-infinite diffusion equations (Crank, 1975), with one equation for each intermittent leaching cycle.

Potassium. The IMT simulation for potassium resulted in release behavior similar to the release of sodium. Flux comparisons and regression statistics shown in Figure 4 indicate that a good agreement was found for all intermittent leaching cases. The IMT model was able to simulate the mean release flux of potassium for all intermittent wetting cases using a single value of effective diffusivity. At the beginning of each intermittent wetting cycle, the IMT simulation captured the increased flux resulting from relaxation of the activity gradient during the previous storage period. However, in the same manner as the sodium simulation, the IMT model was not able to provide a good visual fit for the continuous leaching case. For the continuous leach case, 80% of the total potassium content was released during the 94-day leaching period (Garrabrants et al., 2002), indicating that depletion of potassium from the matrix had occurred.

The potassium activity profiles within the matrix (Figure 8c) show similar curvature to the sodium activity profiles. The core liquid activity relaxed to approach a new equilibrium, reducing the core activity from the initial equilibrium value of 60,000 mg/L to a value of 3,000 mg/L (S6) at the end of IW Cycle 6 in a similar manner as sodium. However, unlike

sodium relaxation, the relaxation of the potassium activity gradient was not quite complete during the shortest storage interval, but took slightly longer to come to complete relaxation. The regressed effective diffusivity for potassium is lower than that of sodium, which may explain the lag in gradient relaxation. Despite the lag in potassium relaxation, there exists the potential to evaluate potassium release using simple analytical diffusion equations applied to each leach period as long as storage periods are assumed greater than 24 h.

Chloride. Chloride simulation using the IMT model was consistent with other highly soluble species. The use of a single effective diffusivity parameter, regressed for the case of intermittent wetting with storage at 23% RH, provided an agreeable simulation of experimental data for the IW cases with storage at 48% and 98% RH (Figure 5). In the case of continuous leaching, the IMT simulation once again did not visually fit the flux curve. Previous leaching characterization studies indicated that nearly 90% of the available chloride was released under a continuous leaching condition (Garrabrants et al., 2002). Assuming that the chloride ion was depleted from the matrix, the 3-D diffusion model shown in Figure 5d was better able to describe the release flux of chloride.

The leaching profiles for chloride followed the pattern common for the other simulated highly soluble species. Figure 8d indicates that the release of chloride during leaching leads to a progression of relaxation plateaus from the initial condition of 9,100 mg/L to 1,000 mg/L (S6) after the storage period of IW Cycle 6. Relaxation of the liquid concentration gradient seems to be nearly complete after the first 24-h storage cycle. This chloride activity relaxation data supports the possibility of using a series of analytical solutions for approximating chloride release from intermittently wetted cement matrices.

Cadmium. Unlike the release of highly soluble species (Na^+, K^+, Cl^-), the release of sparingly soluble species such as heavy metals is largely dependent on the equilibrium activity as a function of solution pH. Thus, the cadmium release simulation shown in Figure 6 utilized the adjusted pH determination approach in the IMT model, accounting for the contribution of alkaline salts on leachate pH. As earlier, the IMT model was able to adequately simulate the release of cadmium for all experimental cases with a single set of parameters.

The value for effective diffusivity regressed using the intermittent wetting case of storage at 23% RH ($D^{\text{obs}}_{23\%}$) was very near the molecular diffusivity (Table 3). However, if the effective diffusivity value was regressed using experimental data from IW cases at other relative humidity levels (48% and 98% RH), a slightly different value was determined. In all, the values of diffusivity for the three IW cases differed by less than an order of magnitude and tended to decrease with increasing relative humidity ($D^{\text{obs}}_{23\%} > D^{\text{obs}}_{48\%} > D^{\text{obs}}_{98\%}$). This trend additionally was observed to be consistent with the relative activity of chloride as a function of intermittent wetting conditions. Thus, these apparent values of diffusivity were considered to reflect complexation of cadmium with chloride, which would increase the activity of chloride in the liquid phases, thus, increasing the observed rate of mass transport through the matrix.

The profile for cadmium activity (Figure 9a) indicates that gradients in cadmium activity became almost completely relaxed during the storage phase of an intermittent wetting cycle. A similar observation was made for the highly soluble species. However, unlike the highly soluble species, the activity profile for the cadmium was influenced by both cadmium gradient relaxation and the relaxation of the pH gradient in the matrix. A profile showing the cadmium solid-phase concentration was more useful for describing the mass-transport process. Figure 9b shows the profile of cadmium in the solid phase very near the surface of the S/S MeO matrix. The IMT model indicated that the mass transport of cadmium followed a moving dissolution front. The value of solid cadmium at the dissolution front was seen to decrease with cycle wetting and storage. Over the six intermittent wetting cycles (~94 days), the simulated penetration of the cadmium dissolution front was approximately 0.06 mm.

Lead. Comparisons of IMT model simulations and experimental data for lead flux are presented in Figure 7 for each of the three intermittent wetting cases and continuous leaching case. Once the effective diffusivity of lead was regressed for the case of intermittent wetting with storage in an atmosphere of 23% relative humidity, the simulations for other cases showed good agreement to experimental data. Although lead, like cadmium, is susceptible to chloride complexation, the effect was less substantial for lead release from this matrix.

In a similar manner to cadmium, the profile of the lead activity in the liquid phase (Figure 9c) was affected by both relaxation of continued lead mass transfer and pH gradients relaxation. If calcium hydroxide alone had been used to provide the pH value, it would be expected that the local activity of pH-dependent species would remain at the initial pore condition until $Ca(OH)_2$ had been depleted. Since the value of the local pH was based on both dissolution of calcium hydroxide and mass transport of highly soluble alkaline salts, the pH and, hence, the activity of lead, within the core of the matrix was not constant, even when $Ca(OH)_2$ solid was present. The profile of solid concentration (Figure 9d) shows that the mass transport of lead was dominated by dissolution from a lead precipitate very near the surface at approximately 0.03 mm. This source of solid-phase lead was a direct result of the solubility of lead as a function of pH and the transport of hydroxide ions. The precipitated lead was replenished by dissolution of solid lead from the core of the matrix. During leaching intervals, the amount of this lead precipitate was decreased due to dissolution near the surface; however, the mechanism for mass transport within the matrix remained intact throughout the intermittent wetting process as a result of continued mass transport over the intermittent storage interval.

Conclusions

The IMT model adequately describes the release of both highly soluble species and trace metals from a cementitious matrix under intermittent wetting conditions without consideration for matrix carbonation. The model parameters for each species were fit for a single case of intermittent wetting with storage at 23% RH and use to assess intermittent wet-

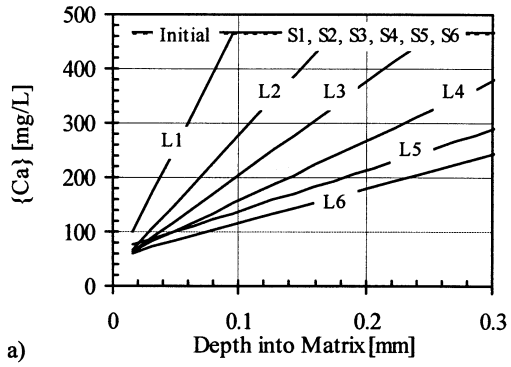

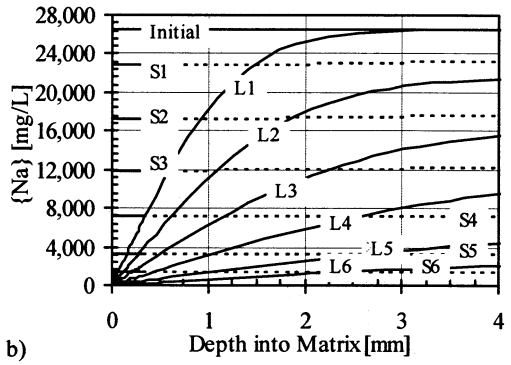

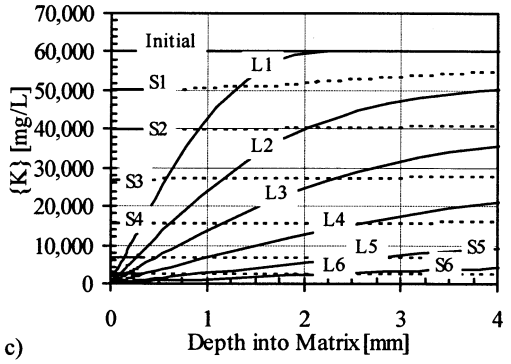

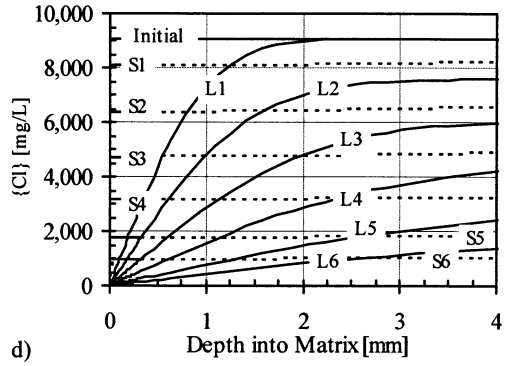

Figure 8. Component activity profiles from IMT model at end of leaching or storage intervals.

(a) Calcium, (b) sodium, (e) potassium, and (d) chloride. Labels "L#" and "S#" equate to "Leaching cycle#" and "Storage cycle#," respectively.

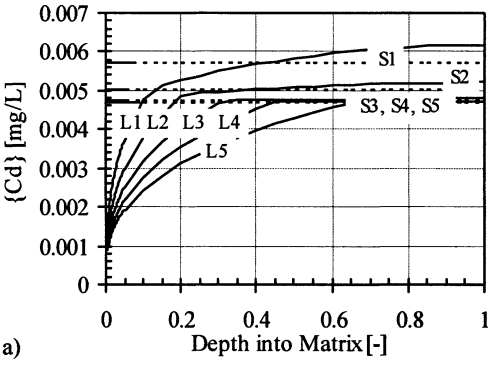

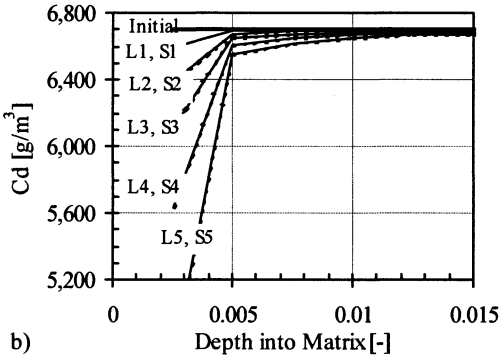

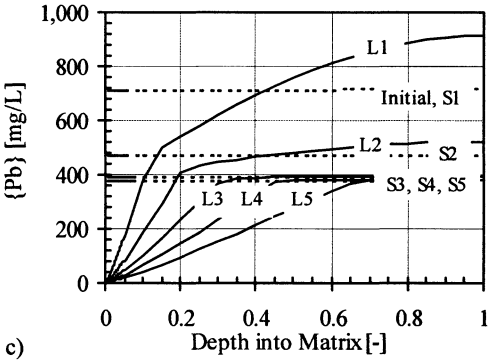

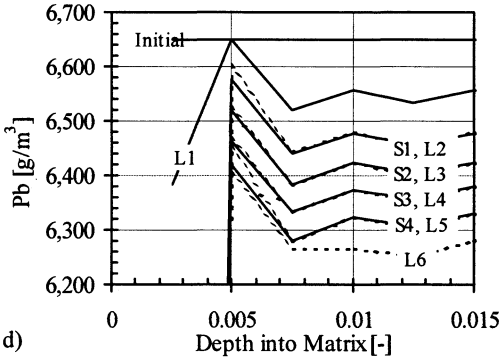

Figure 9. Component activity and concentration profiles from IMT model at end of leaching or storage intervals.

(a) Aqueous phase Cd, (b) aqueous phase Pb, (c) solid phase Cd, and (d) solid phase Pb. Labels "L#" and "S#" equate to "Leaching cycle#" and "Storage cycle#," respectively.

ting release when storage is conducted over a range of constant RH values. It was shown, however, that a 3-D model more accurately describes the release of a highly soluble species under the conditions of continuous leaching. This observation was explained by a depletion of the species from the matrix and the relative application of 1-D and 3-D models to small sample geometries.

Under the assumption that solution pH is provided solely by the dissolution of calcium hydroxide, the IMT model does not accurately simulate the release of hydroxide from the cement matrix and the simulated leachate pH data were consistently lower than the experimental values, especially at the beginning of leaching. Thus, an adjustment was made to account for the diffusion of highly soluble alkaline salts that would (1) be initially present in the pore water at relatively high concentration, (2) suppress the activity of calcium ions in the initial pore solution, (3) increase the local pH values until depletion of the alkaline salt had occurred. After adjustment of the pH equation, the IMT model provided substantially better simulation of leachate pH. Accurate simulation of local pH is important when the release of sparingly soluble species (Pb, Cd) is a concern.

Simulations of activity profiles using the IMT model indicate that the liquid activity profile for highly soluble species such as sodium, potassium, and chloride come to nearly complete relaxation within relatively short storage intervals in all studied intermittent wetting cases. Complete gradient relaxation led to a reduction in species activity at the core of the matrix that progressed with each intermittent leaching cycle. In addition, species release in the subsequent leaching interval was accelerated because the driving force for flux across the solid–leachate interface is maximized at the beginning of subsequent leaching periods. This mechanism can explain why intermittent wetting of highly soluble species leads to more rapid depletion of species activity than observed for continous leaching when the same cumulative duration of leaching is considered. Complete relaxation of the activity profile within a relatively short storage period also allows for the possibility of an alternative modeling approach using a simple semi-infinite diffusion approach over short leaching intervals.

For metal species, liquid activity profiles were influenced by both relaxation of the activity gradients as well as relaxation of the pH gradient within the pore water. Profiles of the solid phase concentration of trace metals were examined to provide an indication of principal mass-transport mechanisms. The IMT model indicated that cadmium release was controlled by the movement of a cadmium dissolution front, while lead mass transfer occurred via dissolution from a spike in solid lead concentration just inside the bulk solid interface.

Application of the IMT model could be used to (1) simulate the release of matrix constituents with a variety of intrinsic solubility behaviors, (2) account for the effect of nonleaching intervals with storage conducted over a range of relative humidity values, (3) point out controlling mechanism for mass transport during leaching and storage intervals, and (4) extend the characteristic release behavior of experimental data over the chosen assessment interval in order to provide the long-term release of COPCs from cementitious materials.

Acknowledgments

This research was supported in part through funding from the Hazardous Substances Management Research Center, an Advanced Technology Center of the New Jersey Commission on Science and Technology and a National Science Foundation Industry/University Cooperative Research Center. Additional support was provided by USDOE (DE-FG26-00NT40938) to the Institute for Responsible Management/Consortium for Risk Evaluation with Stakeholder Participation II (IRM/CRESP II). Opinions, findings, conclusions, or recommendations expressed herein are those of the authors and do not necessarily reflect the views of the DOE or of IRM/CRESP II.

Notation

A = fitted activity model parameter in the Davies relation
$\{A\}$ = $m \times m$ array of equation coefficients used in the Thomas method
a_k = mass activity of species k in liquid phase, mg/L
$a_{k,l}$ = mass activity of species k in leaching solution, mg/L
a_k^{eq} = mass activity of species k in equilibrium with the solid phase, mg/L
B = fitted activity model parameter in the Davies relation
$[b]$ = m-sized vector of known values at time $t = t$ used in the Thomas method
$\{Ca^{2+}\}$ = activity of calcium ions in solution, mg/L
c_k = measured concentration of species k in solution, mg/L
$c_{k,l}$ = measured concentration of species k in the leachate, mg/L
D_k^{eff} = effective diffusivity of species k in the cement matrix, m^2/s
$D_{100\%}^{obs}$ = observed moisture diffusivity at a relative humidity of 100%, m^2/s
d = equivalent half-length of the 3-D matrix in one-dimension, m
F_k = rate of generation or loss of species k in the liquid phase, $kg/m^3 \cdot s$
H = relative humidity
H_{amb} = relative humidity of the ambient atmosphere
H_{surf} = relative humidity at the bulk solid surface
h_c = value of humidity corresponding to the drop in the S-shaped curve of D_H^{obs}
I = ionic strength of the solution, mol/L
$K_{sp}^{Ca(OH)_2}$ = kinetic solubility constant of $Ca(OH)_2$ solid
$K_a^{H_2O}$ = kinetic dissociation constant of water
$\{X\}$ = activity of sodium- and potassium-based alkaline salts in solution, mg/L
L_k = liquid concentration of species k on a global basis, kg/m^3_{matrix}
M_k = molar mass of species k in the liquid phase, g/mol
M_p = molar mass of the species p in the solid phase, g/mol
m = number of simultaneous equations solved in the numerical method
n = exponent characterizing the spread of the drop in the S-shaped curve of D_H^{obs}
$\{OH^-\}$ = activity of hydroxide in solution, mol/L
S_p = solid concentration of species p on a global basis, kg/m^3_{matrix}
$SRSE_j$ = "sum of the residual square errors" for IW cycle j
$SRSE_{sim}$ = "sum of the residual square errors" used as an overall simulation fit statistic
t_j = duration of IW cycle j, s
t_{sim} = duration of the total simulation, s
V = matrix volume, m^3_{matrix}
V_l = volume of the leaching solution, L
w_j = simulation fit criteria weighing function coefficient for cycle j ($w_j = t_j/t_{sim}$)
$[x]$ = m-sized vector of unknown values at time $t = t + dt$ used in the Thomas method
$y_{i,exp}$ = log of the experimental flux at location i, $\log(kg/m^2 \cdot s)$
$y_{i,sim}$ = log of the simulated flux at location i, $\log(kg/m^2 \cdot s)$
z_k = valence charge of species k in the liquid phase

Greek letters

α_o = parameter representing the ratio of D_{min} to D_{max} in the S-shaped curve of D_H^{obs}

β_k = first-order kinetic rate constant for the dissolution of the solid phase p, 1/s
γ_k = single-ion activity coefficient of species k in the liquid phase
ϵ = matrix porosity, m^3_{pore}/m^3_{matrix}
η = mass-transfer coefficient of water vapor across the interfacial boundary layer, $kg/m^2 s$
θ = relative saturation of the matrix pore space, m^3_{liq}/m^3_{pore}
θ^0 = initial value of matrix saturation ($\theta^0 = 1$), m^3_{liq}/m^3_{pore}
θ_{cap} = value of matrix saturation at capillary saturation, m^3_{liq}/m^3_{pore}
θ_{ins} = value of matrix saturation at insular saturation, m^3_{liq}/m^3_{pore}
ρ_{liq} = density of the liquid solution, kg/m^3_{liquid}
σ = matrix surface area exposed to leaching solution or ambient conditions, m^2

Subscripts

i = subscript index for location into the 1-D matrix ($i = 0$ at the bulk surface)
j = subscript index for the IW cycle ($j = 0$ at initial condition)
k = subscript index for liquid-phase species
p = subscript index for solid-phase species

Literature Cited

Barna, R., "Etude de la Diffusion des Polluants dans les Déchets Solidifiés par Liants Hydrauliques," Doctoral Thesis, Institut National des Sciences Appliquées, Lyon, France (1994).

Batchelor, B., and K. Wu, "Effects of Equilibrium Chemistry on Leaching of Contaminants from Stabilized/Solidified Wastes," *Chemistry and Microstructure of Solidified Waste Forms*, R. D. Spence, Ed., Lewis Publishers, Baton Rouge, LA, p. 243 (1993).

Batchelor, B., "Leach Models for Contaminants Immobilized by pH-Dependent Mechanisms," *Environ. Sci. Technol.*, **32**, 1721 (1998).

Bazant, Z. P., and L. J. Najjar, "Drying of Concrete as a Nonlinear Diffusion Problem," *Cem. Concr. Res.*, **1**, 461 (1971).

Bazant, Z. P., and L. J. Najjar, "Nonlinear Water Diffusion in Nonsaturated Concrete," *Matér. Constr.*, **5**, 3 (1972).

Bentz, D. P., and K. K. Hansen, "Preliminary Observations of Water Movement in Cement Pastes During Curing Using X-Ray Absorption," *Cem. Concr. Res.*, **30**, 1157 (2000).

Berendsen, T., "Reuse of Secondary Building Materials in Road Construction," WASCON '97—International Conference on Construction with Waste Materials, Houthem, The Netherlands (1997).

Carde, C., R. François, and J.-M. Torrenti, "Leaching of Both Calcium Hydroxide and C-S-H from Cement Paste: Modeling the Mechanical Behavior," *Cem. Concr. Res.*, **26**, 1257 (1996).

Carde, C., and R. François, "Effect of the Leaching of Calcium Hydroxide from Cement Paste on Mechanical and Physical Properties," *Cem. Concr. Res.*, **27**, 539 (1997a).

Carde, C., and R. François, "Aging Damage Model of Concrete Behavior During the Leaching Process," *Mater. Struct.*, **30**, 465 (1997b).

Carde, C., and R. François, "Modelling the Loss of Strength and Porosity Increase Due to the Leaching of Cement Pastes," *Cem. Concr. Res.*, **21**, 181 (1999).

Carnahan, B., H. A. Luther, and J. O. Wilkes, *Applied Numerical Methods*, Wiley, New York (1969).

Cerný, R., J. Drchalová, and P. Rovnaníková, "The Effects of Thermal Load and Frost Cycles on the Water Transport in Two High-Performance Concrete," *Cem. Concr. Res.*, **31**, 1129 (2001).

Clifton, J. R., J. M. Pommersheim, and K. Snyder, *Long-Term Performance of Engineered Concrete Barriers*, NISTIR 5690, National Institute of Standards and Testing, Building and Fire Research Laboratory, Gaithersburg, MD, p. 22 (1995).

Cocke, D. L., "Exploitation of the Binding Chemistry and Leaching Mechanisms to Improve Solidification/Stabilization of Hazardous Wastes," *Waste Manage.*, **13**, 520 (1993).

Conner, J. R., *Chemical Fixation and Solidification of Hazardous Wastes*, Van Nostrand Reinhold, New York (1990).

Conner, J. R., and S. L. Hoeffner, "The History of Solidification Stabilization Technology," *Crit. Rev. Environ. Sci. Technol.*, **28**, 325 (1998).

Constantinides, A., *Applied Numerical Methods with Personal Computers*, McGraw-Hill, New York (1987).

Crank, J., *The Mathematics of Diffusion*, Oxford Univ. Press, London (1975).

Delagrave, A., M. Pigeon, J. Marchand, and É. Revertégat, "Influence of Chloride Ions and pH Level on the Durability of High Performance Cement Pastes (Part II)," *Cem. Concr. Res.*, **26**, 749 (1996).

Dhir, R. K., P. C. Hewlett, and Y. N. Chan, "Near-Surface Characteristics of Concrete: Prediction of Carbonation Resistance," *Mag. Concr. Res.*, **41**, 137 (1989).

Eighmy, T. T., and W. H. Chesner, *Framework for Evaluating Use of Recycled Materials in the Highway Environment*, FHWA-RD-00-140, Federal Highway Administration, McLean, VA (2001).

Eighmy, T. T., R. A. Cook, D. L. Gress, A. Coviello, J. C. M. Spear, K. Hover, R. Pinto, S. Hobbs, D. Kosson, F. Sanchez, H. van der Sloot, C. Korhonen, and M. Simon, "Use of Accelerated Aging to Predict Behavior of Recycled Materials in Concrete Pavements —Physical and Environmental Comparison of Laboratory-Aged Samples with Field Pavements," *Transp. Res. Rec. 1792*, Transportation Research Board, National Research Council, Washington, DC, **1792**, 118 (2002).

Garrabrants, A. C., F. Sanchez, C. Gervais, P. Moszkowicz, and D. Kosson, "The Effect of Storage in an Inert Atmosphere on the Release of Inorganic Constituents During Intermittent Wetting of a Cement-Based Material," *J. Hazard. Mater.*, **91**, 159 (2002).

Garrabrants, A. C., and D. S. Kosson, "Modeling Moisture Transport from a Cementitious Material During Storage in Reactive and Inert Atmospheres," *Drying Technol.*, **21**, 775 (2003).

Garrabrants, A. C., F. Sanchez, and D. S. Kosson, "Changes in Constituent Equilibrium Leaching and Pore Water Characteristics of Portland Cement Mortar as a Result of Carbonation," *Waste Manage.*, in press (2003).

Gervais, C., A. C. Garrabrants, F. Sanchez, R. Barna, P. Moszkowicz, and D. S. Kosson, "The Effects of Carbonation and Drying During Intermittent Leaching on the Release of Inorganic Constituents from a Cement-Based Matrix," *Cem. Concr. Res.* (2003).

Glasser, F. P., "Chemistry of Cement-Solidified Waste Forms," *Chemistry and Microstructure of Solidified Waste Forms*, R. D. Spence, ed., Lewis Publishers, Baton Rouge, LA, p. 1 (1993).

Hinsenveld, M., "A Shrinking Core Model as a Fundamental Representation of Leaching Mechanisms in Cement Stabilized Waste," PhD Thesis, Univ. of Cincinnati, Cincinnati, OH (1992).

Hinsenveld, M., and P. L. Bishop, "Use of the Shrinking Core/Exposure Model to Describe the Leachability from Cement Stabilized Wastes," *Stabilization and Solidification of Hazardous, Radioactive, and Mixed Wastes, ASTM STP 1240*, 3rd ed., T. M. Gilliam and C. C. Wiles, eds., American Society for Testing and Materials, Philadelphia (1996).

Jansegers, E., "The Use of MSWI Bottom Ash in Hollow Construction Materials," WASCON '97—International Conference on Construction with Waste Materials, Houthem, The Netherlands (1997).

Johannesson, B. F., "Diffusion of a Mixture of Cations and Anions Dissolved in Water," *Cem. Concr. Res.*, **29**, 1261 (1999).

Johnson, R. A., and G. K. Bhattacharyya, *Statistics — Principles and Methods*, Wiley, New York (1992).

Kayyali, O. A., and M. S. Qasrawi, "Chloride Binding Capacity in Cement-Fly-Ash Pastes," *J. Mater. Civ. Eng.*, **4**, 16 (1992).

Kim, I., and B. Batchelor, "Empirical Partitioning Leach Model for Solidified/Stabilized Wastes," *J. Environ. Eng.*, **127**, 188 (2001).

Kjellsen, K. O., and H. M. Jennings, "Observations of Microcracking in Cement Paste Upon Drying and Rewetting by Environmental Scanning Electron Microscopy," *Adv. Cem.-Based Mater.*, **3**, 14 (1996).

Klemm, A. J., and P. Klemm, "The Effects of the Alternate Freezing and Thawing Cycles on the Pore Structure of Cementitious Composites Modified by MHEC and PVA," *Build. Environ.*, **32**, 509 (1997).

Klich, I., B. Batchelor, L. P. Wilding, and L. R. Drees, "Mineralogical Alterations that Affect the Durability and Metals Containment of Aged Solidified and Stabilized Wastes," *Cem. Concr. Res.*, **29**, 1433 (1999).

Kosson, D. S., H. A. van der Sloot, and T. T. Eighmy, "An Approach for Estimating of Contaminant Release During Utilization and Disposal of Municipal Waste Combustion Residues," *J. Hazard. Mater.*, **47**, 43 (1996).
Landsberger, S., "Nuclear Techniques and the Disposal of Non-Radioactive Solid Waste," *IAEA Bull.*, **35**, 14 (1993).
Lange, L. C., C. D. Hills, and A. B. Poole, "Preliminary Investigation into the Effects of Carbonation on Cement-Solidified Hazardous Wastes," *Environ. Sci. Technol.*, **30**, 25 (1996).
Lide, D. R., ed., *CRC Handbook of Chemistry and Physics*, CRC Press, Boca Raton, FL (1996).
Macías, A., A. Kindness, and F. P. Glasser, "Impact of Carbon Dioxide on the Immobilization Potential of Cemented Wastes: Chromium," *Cem. Concr. Res.*, **27**, 215 (1997).
Mollah, M. Y. A., R. K. Vempati, T.-C. Lin, and D. L. Cocke, "The Interfacial Chemistry of Solidification/Stabilization of Metals in Cement and Pozzolanic Material Systems," *Waste Manage.*, **15**, 137 (1995).
Mollah, Y. M., T. R. Hess, Y.-N. Tsai, and D. L. Cocke, "FTIR and XPS Investigations of the Effects of Carbonation on the Solidification/Stabilization of Cement Based System—Portland Type V with Zinc," *Cem. Concr. Res.*, **23**, 773 (1993).
Morel, F., and J. G. Hering, *Principles and Applications of Aquatic Chemistry*, Wiley, New York (1993).
Moszkowicz, P., R. Barna, J. Méhu, H. van der Sloot, and D. Hoede, "Leaching Behavior Assessment of Wastes Solidified with Hydraulic Binders: Critical Study of Diffusional Approach," *Environmental Aspects of Construction with Waste Materials*, J. J. J. M. Goumans, H. A. van der Sloot, and T. G. Aalbers, eds., Elsevier Science, Amsterdam, p. 421 (1994).
Moszkowicz, P., R. Barna, F. Sanchez, H. R. Bae, and J. Méhu, "Models for Leaching of Porous Materials," WASCON '97—International Conference on Construction with Waste Materials, Houtham, The Netherlands (1997).
Moszkowicz, P., F. Sanchez, R. Barna, and J. Méhu, "Pollutants Leaching Behaviour from Solidified Wastes: A Selection of Adapted Various Models," *Talanta*, **46**, 375 (1998).
Nishigaki, M., "Producing Permeable Blocks and Pavement Bricks from Molten Slag," *Waste Manage.*, **20**, 185 (2000).
Papadakis, V. G., C. G. Vayenas, and M. N. Fardis, "Reaction Engineering Approach to the Problem of Concrete Carbonation," *AIChE J.*, **35**, 1639 (1989).
Papadakis, V. G., C. G. Vayenas, and M. N. Fardis, "Experimental Investigation and Mathematical Modeling of the Concrete Carbonation Problem," *Chem. Eng. Sci.*, **46**, 1333 (1991).
Park, J.-Y., and B. Batchelor, "Prediction of Chemical Speciation in Stabilized/Solidified Wastes Using a General Chemical Equilibrium Model. Part I. Chemical Representation of Cementitious Binders," *Cem. Concr. Res.*, **29**, 361 (1999a).
Park, J.-Y., and B. Batchelor, "Prediction of Chemical Speciation in Stabilized/Solidified Wastes Using a General Chemical Equilibrium Model. Part II. Doped Waste Contaminants in Cement Porewaters," *Cem. Concr. Res.*, **29**, 99 (1999b).
Park, J.-Y., and B. Batchelor, "A Multi-Component Numerical Leach Model Coupled with a General Chemical Speciation Code," *Water Res.*, **36**, 156 (2002).
Patankar, S. V., *Numerical Heat Transfer and Fluid Flow*, Hemisphere, New York (1980).
Penev, D., and M. Kawamura, "Moisture Diffusion in Soil-Cement Mixtures and Compacted Lean Concrete," *Cem. Concr. Res.*, **21**, 137 (1991).
Pitzer, K. S., "Theory: Ion Interaction Approach," *Activity Coefficients in Electrolyte Solutions*, R. M. Pytkowicz, ed., CRC Press, Boca Raton, FL (1979).
Rogers, J. A., and M. Kaviany, "Funicular and Evaporative-Front Regimes in Convective Drying of Granular Beds," *Int. J. Heat Mass Transfer*, **35**, 469 (1992).
Sakata, K., "A Study on Moisture Diffusion in Drying and Drying Shrinkage of Concrete," *Cem. Concr. Res.*, **13**, 216 (1983).
Sanchez, F., "Etude de la Lixiviation de Milieux Poreux Contenant des Espèces Solubles: Application au cas des Déchets Solidifiés par Liants Hydrauliques," Doctoral Thesis, Institut National des Sciences Appliquées, Lyon, France, 269 pp. (1996).
Sanchez, F., R. Barna, A. C. Garrabrants, D. S. Kosson, and P. Moszkowicz, "Environmental Assessment of a Cement-Based Solidified Soil Contaminated with Lead," *Chem. Eng. Sci.*, **55**, 113 (2000).
Sanchez, F., C. Gervais, A. C. Garrabrants, R. Barna, and D. S. Kosson, "Leaching of Inorganic Contaminants from Cement-Based Waste Materials as a Result of Carbonation During Intermittent Wetting," *Waste Manage.*, **22**, 249 (2001).
Sanchez, F., A. C. Garrabrants, and D. S. Kosson, "Effects of Intermittent Wetting on Concentration Profiles and Release from a Cement-Based Waste Matrix," *Environ. Eng. Sci.*, **20**, 135 (2003).
Šelih, J., A. C. M. Sousa, and T. W. Bremner, "Moisture Transport in Initially Fully Saturated Concrete During Drying," *Transp. Porous Media*, **24**, 81 (1996).
Stumm, W., and J. J. Morgan, *Aquatic Chemistry: Chemical Equilibria and Rates in Natural Waters*, Wiley-Interscience, New York (1996).
Manuscript received Sept. 19, 2002, and revision received Dec. 20, 2002.